JOURNAL OF PROPULSION AND POWER
Vol. 10, No. 5, Sept.–Oct. 1994

Design of Axisymmetric Channels with Rotational Flow

M. Koumandakis,* V. Dedoussis,† P. Chaviaropoulos,‡ and K. D. Papailiou§
National Technical University of Athens, 157 10 Athens, Greece

The purpose of this article is to present an inverse subsonic inviscid method for the design of axisymmetric channels, with rotational flow. The rotational character of the flow is due to prescribed total enthalpy, entropy, and/or swirl gradients along the inlet of the channel. The method is based on a potential function/stream function formulation. The Clebsch transformation is employed to decompose the meridional velocity vector into a potential and a rotational part. The rotational part is shown to be proportional to the total enthalpy gradient, the coefficient of proportionality being the drift function. A body-fitted coordinate transformation is employed to map the sought boundaries on the (ϕ, ψ) space. The governing equation for the magnitude of the meridional velocity component is derived by treating the inverse problem on the (ϕ, ψ) space as a purely geometric one, employing differential geometry principles. The (meridional) velocity equation is coupled in a nonlinear manner with a transport equation for the drift function and with the geometry via the radial coordinate. The integration of the governing equations is performed on an auxiliary computational grid using a simple iterative scheme. The geometry, in particular, is determined by integrating Frenet equations along the grid lines. The present design method has been applied successfully to the "reproduction" of two "real-life" geometries concerning the annular duct of a two-stage axial compressor as well as a radial one.

Nomenclature

a, b, c, d, e, f = velocity Eq. (24) coefficients
c_p, c_v = specific heats
G_{ij} = metrics tensor of computational (ξ, η) coordinate system
g^{ij} = conjugate metrics tensor of natural (ϕ, ψ) coordinate system
$\vec{g}^i$ = contravariant base vector of natural (ϕ, ψ) coordinate system
h = enthalpy
$\vec{k}$ = unit base vector in the peripheral direction
$\vec{L}$ = position vector
M = Mach number
s = entropy
T = temperature
$\vec{V}$ = velocity vector
(x, r) = meridional plane (physical) Cartesian coordinate system
α = drift function
α_h, α_s, α_u = Clebsch decomposition coefficients associated with enthalpy, entropy, and swirl gradients
β = angle between $\nabla_m\phi$, $\nabla_m\psi$
Γ^l_{ij} = Christoffel symbol of second kind
γ = specific heats ratio
Θ_1 = angle between η = const lines and axis of channel, x axis
κ_1 = signed curvature of η = const lines
λ = entropy gradient coefficient
μ = swirl gradient coefficient
(ξ, η) = orthogonal computational coordinate system
ρ = density
$\tilde{\rho}$ ($=r\rho$) = modified density
(ϕ, ψ) = potential function, stream function natural coordinate system
$\vec{\Omega}$ = vorticity vector

Subscripts
i, j, l, q ($=1, 2$) = covariant tensor indices
m = meridional component
o = known position indicator
ref = reference quantity
t = total quantity
u = peripheral component
ξ, η, ϕ, ψ = partial derivatives with respect to ξ, η, ϕ, or ψ

Superscripts
i, j, l, q ($=1, 2$) = contravariant tensor indices

Introduction

A CENTRAL issue in applied aerodynamics is the problem of determining the shape of the walls of an aerodynamic component on which the pressure (or velocity in inviscid flows) distribution is prescribed. This inverse problem is usually referred to as the "target pressure" one. Over the years quite a few methods have been developed for its solution. First attempts addressed the design of airfoils in incompressible potential flows using analytical conformal mapping techniques.[1] The cornerstone, however, of inverse approaches is the method developed by Stanitz[2] in which the governing equations are transformed employing the potential function ϕ and the stream function ψ as "natural" body-fitted coordinates. The method is very robust because it exploits the fact that solid boundaries are streamlines, which implicitly defines the domain of integration of the unknown, sought, geometry on the (ϕ, ψ) space. The method of Stanitz was originally proposed for the design of two-dimensional channels with either incompressible or compressible (subsonic) potential flow. Due to its flexibility, Stanitz's approach was extended to the design of axisymmetric internal flow configurations,[3] turbo-

Presented as Paper 93-3117 at the AIAA 24th Fluid Dynamics Conference, Orlando, FL, July 6–9, 1993; received July 19, 1993; revision received Jan. 31, 1994; accepted for publication Feb. 15, 1994.

*Undergraduate Student, Laboratory of Thermal Turbomachines, P.O. Box 64069.

†Research Associate, Laboratory of Thermal Turbomachines, P.O. Box 64069; currently Lecturer, Department of Industrial Management, University of Piraeus, Piraeus 18534, Greece. Member AIAA.

‡Research Engineer, Laboratory of Thermal Turbomachines, P.O. Box 64069.

§Professor, Department of Mechanical Engineering, Laboratory of Thermal Turbomachines, P.O. Box 64069. Member AIAA.

machinery planar and axisymmetric nonrotating or rotating blading,[4-6] and to isolated airfoils.[7]

During the last decade solution of the target pressure problem and its variants, where additional desirable design characteristics, incorporated as "flow or geometry constraints," may be prescribed, is tackled by coupling aerodynamic analysis tools with numerical optimization (minimization) schemes. These methods provide the design geometry via an iteration loop between the analysis, direct, problem solution, and the appropriate update of the judiciously guessed geometry. Depending on the governing equations solved by the analysis code (e.g., full potential, Euler or Navier-Stokes), "optimum" design configurations for potential,[8] rotational,[9] or viscous flow,[10] respectively, are achieved. Although the speed of computation has increased enormously, numerical optimization techniques are still much more expensive (but more flexible) than the traditional potential/stream function inverse design formulations. To the benefit of the latter approach is that, through the utilization of natural coordinates, it enables the treatment of the inverse problem as a geometrical problem rather than a flow one. This provides a better insight and theoretical understanding of the inverse design problem as such.[11,12] Exhaustive presentation of the advantages and disadvantages of various design methods is beyond the scope of the present work. Complete discussion of aerodynamic shape design methods can be found in the review papers of Labrujere and Slooff[13] and Dulikravich.[14]

Potential/stream function inverse methods were developed for potential flows only. Rotational flows have received only limited attention mainly because of the breakdown of the concept of the potential function. The difficulty can be circumvented using the Clebsch formulation[15] to decompose the velocity vector into a gradient-type "potential" part and another rotational part. The present authors[16] used this technique to solve the rotational two-dimensional inverse problem for internal flow configurations. In this article, our previous work is extended to the design of axisymmetric channels with highly rotational flows. The rotational character of the (meridional plane) flow is due to total enthalpy, entropy, and/or swirl level variations of the different streamlines. Such flow conditions are usually encountered in turbomachine components downstream of highly loaded rotors. The efficient design of such components results in improved overall performance of the machine.

Unlike other axisymmetric inverse methods,[3,17] where governing equations are derived by manipulating the basic flow equations themselves, in our method the equation for the magnitude of the meridional velocity component is derived using the defining relations of the potential and the stream function, and employing differential geometry principles for the mapping-transformation of the physical (x, r) space on the natural (ϕ, ψ) space. This nonlinear partial differential equation (PDE) for the meridional velocity is solved in conjunction with a transport equation for the "drift function" (the sum of the rotational character scalar coefficients involved in the Clebsch decomposition). A difficulty inherently associated with axisymmetric flow conditions is that the velocity equation is coupled with the radial physical coordinate. This implies that the flow and geometry calculations are coupled. For potential flows only, the present authors were able to avoid the flow-geometry calculations coupling, by treating the axisymmetric design problem as a particular case of the genuinely three-dimensional one.[11]

In the present work the numerical integration of the equations is carried out on an auxiliary (ξ, η) computational domain, with η = const lines coinciding with meridional streamlines. Prescribed meridional velocity distribution along the solid walls, instead of the target pressure, as well as prescribed inflow kinematic and thermodynamic properties are used as boundary conditions. The geometry of the duct is determined through the integration of Frenet equations along the computational grid lines.

To validate the method calculations for two "real-life" axisymmetric annular ducts were carried out. The favorable comparisons between inverse results and those of a direct analysis code, indicate the reliability of the method.

Assumptions and Basic Equations

The design method proposed in this article concerns steady, subsonic, inviscid, and adiabatic duct flows of a perfect gas with axial symmetry. Although gradients in the peripheral direction vanish, nonzero peripheral velocity component V_u is assumed. The entropy as well as the total enthalpy level of different stream surfaces (or meridional plane streamlines) may be different.

Under those assumptions the conservation laws of fluid mechanics read

Continuity equation

$$\nabla_m \cdot (\rho \vec{V}_m) = 0 \tag{1}$$

Momentum equation

Meridional (x, r) plane component

$$\vec{V}_m \times \vec{\Omega}_u = \nabla_m h_t - T\nabla_m s - (V_u/r)\nabla_m(rV_u) \tag{2}$$

Peripheral component

$$\vec{V}_m \cdot \nabla_m(rV_u) = 0 \tag{3}$$

Energy equation

$$\vec{V}_m \cdot \nabla_m h_t = 0 \tag{4}$$

where subscript m denotes properties on the meridional plane, whereas subscript u denotes properties along the peripheral direction.

Rearranging Eq. (2) and taking into account Eqs. (3) and (4), we get the entropy conservation law:

$$\vec{V}_m \cdot \nabla_m s = 0 \tag{5}$$

The above system of equations is supplemented by the following density equation:

$$(\rho/\rho_{\text{ref}})^{\gamma-1} = (h/h_{\text{ref}})\exp\{-[(s - s_{\text{ref}})/c_v]\} \tag{6}$$

where subscript ref denotes reference conditions, and γ is the ratio of specific heats c_p/c_v.

The perfect gas assumption implies that the enthalpy is proportional to the temperature, i.e., $dh = c_p\, dT$. It is also noted that the total (stagnation) enthalpy is defined as

$$h_t = h + \tfrac{1}{2}(V_m^2 + V_u^2) \tag{7}$$

Potential-Type/Stream Function Formulation

The purpose of this section is to present and discuss the natural, potential stream function coordinates employed in the present inverse design method.

Stream Function

A stream function on the meridional plane is used that is defined as

$$\bar{\rho}\vec{V}_m = \nabla_m\psi \times \vec{k}, \qquad \bar{\rho} = r\rho \tag{8}$$

As usual, the stream function is defined in such a way so that the continuity Eq. (1) is satisfied identically. The definition of the stream function in axisymmetric flows is analogous to

the usual two-dimensional one, with the exception that the density is replaced by the term $\tilde{\rho}$.

Clebsch Formulation

Clebsch formulation[15] is used to decompose the meridional velocity vector to an irrotational and a rotational part. The rotational part is expressed as a linear combination of $\nabla_m h_t$, $\nabla_m s$, and $\nabla_m(rV_u)$, which are responsible for the rotational character of the flow (peripheral vorticity component).

The Clebsch decomposition of the meridional velocity vector reads

$$\vec{V}_m = \nabla_m\phi + \alpha_h\nabla_m h_t + \alpha_s\nabla_m s + \alpha_u\nabla_m(rV_u) \tag{9}$$

where ϕ is the meridional plane potential function.

Equations (3–5) indicate that $\nabla_m h_t$, $\nabla_m s$, and $\nabla_m(rV_u)$, being normal to $\vec{V}_m$, are parallel with one another. Assuming that the total enthalpy is a primary variable, the effect of the entropy and swirl gradients can be expressed as

$$\nabla_m s = \lambda\nabla_m h_t \tag{10}$$

$$\nabla_m(rV_u) = \mu\nabla_m h_t \tag{11}$$

Applying the meridional curl operator on Eqs. (10) and (11) it is seen that

$$\nabla_m\lambda \times \nabla_m h_t = 0 \tag{12}$$

$$\nabla_m\mu \times \nabla_m h_t = 0 \tag{13}$$

Therefore, $\nabla_m\lambda$ and $\nabla_m\mu$ being parallel to $\nabla_m h_t$, are both normal to the meridional streamlines, i.e.,

$$\vec{V}_m\cdot\nabla_m\lambda = 0 \tag{14}$$

$$\vec{V}_m\cdot\nabla_m\mu = 0 \tag{15}$$

Transport Eqs. (14) and (15) simply state that λ and μ are conserved along, i.e., remain constant on, the meridional plane streamlines.

Using Eqs. (10) and (11), Eq. (9) is written equivalently as

$$\vec{V}_m = \nabla_m\phi + \alpha\nabla_m h_t \tag{16}$$

The coefficient α

$$\alpha \equiv \alpha_h + \alpha_s\lambda + \alpha_u\mu \tag{17}$$

Introducing Eqs. (10), (11), and (16) into the meridional momentum Eq. (2), and using the defining relation for the peripheral vorticity component, i.e., $\vec{\Omega}_u = \nabla_m \times \vec{V}_m$, the following transport equation for the drift function is derived:

$$\vec{V}_m\cdot\nabla_m\alpha = T\lambda + (V_u/r)\mu - 1 \tag{18}$$

Natural (ϕ, ψ) Curvilinear Coordinate System

The potential function and the stream function, i.e., the natural coordinates, on the meridional plane, are considered to be the independent variables. The defining Eqs. (8) and (16) provide the contravariant base of the (ϕ, ψ) coordinate system. Associating coordinate indices 1 and 2 with the ϕ and ψ coordinates, respectively, the contravariant base reads

$$\vec{g}^1 \equiv \nabla_m\phi = \vec{V}_m - \alpha\nabla_m h_t \tag{19}$$

$$\vec{g}^2 \equiv \nabla_m\psi = \vec{k} \times \tilde{\rho}\vec{V}_m \tag{20}$$

The dot product $\nabla_m\phi\cdot\nabla_m\psi$ is definitely nonzero since both $\nabla_m h_t$ and $\nabla_m\psi$ are normal to $\vec{V}_m$ [refer to Eqs. (4) and (8), respectively]. This indicates that, unlike irrotational flow, in the present rotational one the (ϕ, ψ) coordinate system is nonorthogonal.

The conjugate (contravariant) metrics of the (ϕ, ψ) system, which actually define the body-fitted physical (x, r) space to the natural (ϕ, ψ) space transformation, are evaluated via the defining relations and Eqs. (19) and (20) as follows:

$$g^{11} \equiv \vec{g}^1\cdot\vec{g}^1 = V_m^2 + \alpha^2|\nabla_m h_t|^2 = (V_m^2/\sin^2\beta) \tag{21}$$

$$g^{22} \equiv \vec{g}^2\cdot\vec{g}^2 = (\tilde{\rho}V_m)^2 \tag{22}$$

$$g^{12} = g^{21} \equiv \vec{g}^1\cdot\vec{g}^2 = -\alpha\tilde{\rho}V_m|\nabla_m h_t| = (\tilde{\rho}V_m^2/\tan\beta) \tag{23}$$

Noting that h_t is constant along the streamlines [see Eq. (4)], Eq. (23) provides the following expression for the coordinate angle:

$$\tan\beta = -(1/\alpha\tilde{\rho}(h_t)_\psi) \tag{24}$$

Governing Equations

The equations that are actually solved by the present inverse method are presented in this section.

Velocity Equation

An equation for the magnitude of the meridional velocity component is obtained from the zero-curvature metrics compatibility condition, which has to be satisfied by any parametrization of the physical space, including the (ϕ, ψ) natural coordinates one. This procedure, which treats the inverse problem as a geometrical rather than a flow one, proved to be quite efficient in several inverse design applications in two[7,16] and three dimensions.[11,18]

From the analysis presented in the previous section it is observed that in the present axisymmetric formulation the metrics expressions are entirely analogous to those of the two-dimensional one, with the only exception being that the thermodynamic density has to be replaced by the modified density function $\tilde{\rho}$ ($=r\rho$). The relevant meridional velocity equation, therefore, is identical to the two-dimensional velocity equation,[16] provided that ρ is replaced by $\tilde{\rho}$. Thus

$$a(\not{r}\, V_m)_{\phi\phi} + b(\not{r}\, V_m)_{\phi\psi} + c(\not{r}\, V_m)_{\psi\psi} + d(\not{r}\, V_m)_\phi + e(\not{r}\, V_m)_\psi = f \tag{25}$$

where

$$a(\tilde{\rho}, \beta) = (1/\sin^2\beta)$$

$$b(\tilde{\rho}, \beta) = (2\tilde{\rho}/\tan\beta)$$

$$c(\tilde{\rho}, \beta) = \tilde{\rho}^2$$

$$d(\tilde{\rho}, \beta) = -(1/\sin^2\beta)[(\not{r}\,\tilde{\rho})_\phi + \tilde{\rho}\beta_\psi + (2/\tan\beta)\beta_\phi]$$

$$e(\tilde{\rho}, \beta) = \tilde{\rho}^2(\not{r}\,\tilde{\rho})_\psi - (\tilde{\rho}/\sin^2\beta)\beta_\phi$$

$$f(\tilde{\rho}, \beta) = -\frac{1}{\sin^2\beta}(\not{r}\,\tilde{\rho})_{\phi\phi} - \frac{\tilde{\rho}}{\tan\beta}(\not{r}\,\tilde{\rho})_{\phi\psi} + \frac{(\not{r}\,\tilde{\rho})_\phi}{\sin^2\beta} \times \left[(\not{r}\,\tilde{\rho})_\phi + \tilde{\rho}\beta_\psi + \frac{3}{\tan\beta}\beta_\phi\right] - \frac{1}{\sin^2\beta\tan\beta}\beta_{\phi\phi} - \frac{\tilde{\rho}}{\sin^2\beta}\beta_{\phi\psi} + \frac{2\tilde{\rho}}{\sin^2\beta\tan\beta}\beta_\phi\beta_\psi + \frac{2\cos^2\beta + 1}{\sin^4\beta}(\beta_\phi)^2$$

The nonlinear elliptic type second-order PDE for the meridional velocity component V_m, Eq. (25), is the main governing equation of the flowfield. For irrotational axisymmetric flows, where potential lines are normal to the streamlines on the meridional plane, i.e., $\beta = 90$ deg, Eq. (25) is identical

to those of Stanitz[17] and Nelson and Yang[3] for compressible and incompressible flows, respectively.

The coefficients of Eq. (25) are functions of $\bar{\rho}$ and β. The function $\bar{\rho}$ defined as the product of the thermodynamic density ρ, and the radial coordinate r is a function of the (unknown) design geometry sought. This implies that in contrast to the two-dimensional case, the flow and geometry solution procedures cannot be separated and carried out in an independent manner. The need of treating the axisymmetric inverse design problem as a coupled flowfield-geometry problem is evident.

To close the design problem one has to provide equations for $\bar{\rho}$ (or for ρ), for the geometry (r coordinate) and for β. The thermodynamic density is evaluated using Eq. (6), whereas the coordinate angle is evaluated in terms of the drift function using Eq. (24).

Transport Equation for the Drift Function

The drift function is calculated from the transport Eq. (18). In the (ϕ, ψ) coordinate system this transport equation becomes

$$V_m^2 \alpha_\phi = T\lambda + (V_u/r)\mu - 1 \tag{26}$$

It is interesting to note that the drift function Eq. (26) is also coupled to the geometry. This coupling is both implicit and explicit. Equation (26) is implicitly coupled to the geometry solution via the meridional velocity field (which controls the transport rate of the drift function), and explicitly via the nonzero peripheral velocity term on its right side.

The total enthalpy as well as the entropy and the swirl are prescribed at the inlet section as $h_t = h_t(\psi)$, $s = s(\psi)$ and $rV_u = rV_u(\psi)$, implicitly setting the level of the rotational character, peripheral vorticity, of the flow considered. Taking also into account that h_t, s, and rV_u are conserved along the meridional streamlines, i.e., on ψ = const lines [refer to Eqs. (3–5)], it is concluded that h_t, s, and rV_u are known, set up a priori, on the entire flow domain. The distributions $\lambda = \lambda(\psi)$ and $\mu = \mu(\psi)$ determined at the inlet via the defining Eqs. (10) and (11) of λ and μ as proportionality coefficients between the parallel vectors $\nabla_m s$, $\nabla_m h_t$, and $\nabla_m(rV_u)$, $\nabla_m h_t$, respectively, are also known a priori throughout the flowfield, simply because λ and μ are conserved on the meridional streamlines. With the exception of the temperature [which is related via Eq. (7) to the total enthalpy and velocity field] and the radial coordinate, the right side of Eq. (26) represents a known function of the ψ coordinate.

Geometry Equations

In the previous section it has been emphasized that in the axisymmetric case the flowfield and geometry solutions are inherently coupled via the radial coordinate. The calculation of the geometry as well as the integration of the flowfield equations are carried out on an auxiliary computational (ξ, η) grid with η = const lines corresponding to the meridional streamlines ψ = const lines. [The (ϕ, ψ) domain of integration and the (ξ, η) grid are discussed in the following sections.] The geometry of the axisymmetric channel, i.e., its typical meridional section, is determined by integrating Frenet equations of η = const and/or ξ = const lines in the physical plane. In the case of (two-dimensional) meridional plane lines the integration of Frenet equations, e.g., of η = const lines (meridional streamlines), is simplified, giving the following relations for their Cartesian coordinates x and r, the axial and radial distance of a point, respectively:

$$x_1 = x_{1o} + \int_{\xi_o}^{\xi} \cos\Theta_1 \sqrt{G_{11}}\, d\xi \tag{27}$$

$$r_1 = r_{1o} + \int_{\xi_o}^{\xi} \sin\Theta_1 \sqrt{G_{11}}\, d\xi \tag{28}$$

with Θ_1, given by

$$\Theta_1 = \Theta_{1o} + \int_{\xi_o}^{\xi} \kappa_1 \sqrt{G_{11}}\, d\xi \tag{29}$$

Relations analogous to Eqs. (27–29) hold for the ξ = const lines.

In Eq. (29), κ_1 is the signed curvature of η = const lines. For the general nonorthogonal (ξ, η) coordinate system κ_1 is

$$\kappa_1 = \frac{\Gamma_{11}^2}{G_{11}|\Gamma_{11}^2|}\left[(\Gamma_{11}^2)^2 G_{22} - [\Gamma_{11}^2 - \tfrac{1}{2}(\sqrt{G_{11}})_\eta]^2 G_{11}\right]^{1/2} \tag{30}$$

where the Christoffel symbols and the metrics with capital letters refer to the (ξ, η) coordinate system. The latter are related to those of the (ϕ, ψ) system, implicitly defined by the relations (21–24), through the following generalized tensor transformation[19]:

$$G_{ij} = \frac{\partial x^q}{\partial \bar{x}^i}\frac{\partial x^l}{\partial \bar{x}^j} g_{ql}$$

$$(x^1 = \phi, \quad x^2 = \psi, \quad \bar{x}^1 = \xi, \quad \bar{x}^2 = \eta) \tag{31}$$

with $i, j, l, q = 1, 2$.

In the above relation the g_{ql} metrics are related to the flow quantities, whereas the $\partial x^q/\partial \bar{x}^l$ derivatives are known functions of the (ϕ, ψ) to (ξ, η) coordinate transformation. By definition, the Christoffel symbols are functions of the metrics and their derivatives.

(ϕ, ψ) Domain of Integration and Boundary Conditions

The inverse problem has a unique solution on the (ϕ, ψ) plane provided that appropriate boundary conditions are specified for the velocity (25), the drift function (26), and the geometry Eqs. (27–29).

α is governed by the first-order ordinary differential Eq. (26), for which initial boundary conditions are required along the inlet section. α, which controls the size of $\tan\beta$, i.e., the local skewness of the (ϕ, ψ) coordinate system, is specified as an arbitrary constant along the inlet section without affecting the final flowfield solution. h_t, s, and rV_u distributions are also prescribed along the inlet section, implicitly specifying the level of the incoming (peripheral) vorticity as well as the thermodynamic density.

Initial conditions are also required for the integration of the geometry Eqs. (27–29). The (x_o, r_o) coordinates and the corresponding Θ_{1o} angle are fixed at a preselected location. For undisturbed inlet conditions Θ_{1o} is arbitrarily set to zero.

The velocity equation, being of elliptic type, requires boundary conditions all around the integration domain. In the design of axisymmetric annular channels (which concerns the present work), the designer prescribes the meridional velocity magnitude as a function of the solid walls arc lengths, i.e., $V_m = V_m(L)$. In both irrotational and rotational flows the potential ϕ is related to the arc length L on the solid wall (streamlines) via the relation $d\phi = \vec{V}_m \cdot d\vec{L}$. It is obvious, therefore, that the prescribed $V_m = V_m(L)$ distribution corresponds to an easily obtainable $V_m = V_m(\phi)$ distribution, where ϕ is determined to within an arbitrary constant. Without loss of generality the constant of integration for the inner wall velocity distribution could be considered to be zero. On the other hand, the constant of integration of the outer wall velocity distribution is calculated by integrating along the inlet the expression

$$d\phi = -\alpha\, dh_t \tag{32}$$

Equation (32) is derived by requiring the dot product $\vec{V}_m \cdot d\vec{L}$, $d\vec{L}$ being the infinitesimal vector tangential to the inlet sec-

tion, to be zero. Namely, one requires the inlet section to be normal to the (meridional) flow or to the streamlines, ψ = const lines.

The meridional velocity magnitude is also prescribed along the inlet and outlet sections. On these sections the stream function definition yields $d\psi = \bar{\rho}\bar{V}_m \cdot d\bar{L}$ and, consequently, $V_m = V_m(\psi)$. A trapezoidal (ϕ, ψ) domain of integration is therefore defined, for which velocity boundary conditions of Dirichlet type are prescribed on the complete boundary while thermodynamic and geometric boundary conditions are specified on the inlet section.

In general, the inner and outer wall meridional velocity distributions could be specified by the designer in an arbitrary way. Specifying the shape of both the inlet and outlet sections is in general incompatible with the defined (ϕ, ψ) domain of integration. The designer may specify a desirable property for the inlet section [see Eq. (32)], but should leave the outlet section free to adjust itself to a shape compatible with both the defined (ϕ, ψ) domain of integration and the calculated flowfield. In the present work no desirable property is specified for the outlet section. The outlet section is simply assumed to be a straight line on the (ϕ, ψ) plane.

Numerical Method

The defined (ϕ, ψ) domain of integration is discretized assuming uniformly distributed ψ = const lines. An auxiliary numerical transformation[20] is employed that maps the trapezoidal (ϕ, ψ) domain to a rectangular one with square unit cells in a computational (ξ, η) plane. η = const lines correspond to ψ = const lines, i.e., $\psi_\xi = 0$. Limiting values of ξ = const family lines correspond to the inlet and outlet sections. Within the iterative solution procedure the specified (ϕ, ψ) domain of integration remains unchanged. It is noted that if one specifies desirable geometric properties for both the inlet and outlet sections, the (ϕ, ψ) domain of integration and inevitably the (ϕ, ψ) to (ξ, η) mapping should be appropriately updated within the iterative solution procedure. The latter strategy had been adopted in our previous work[16] concerning the design of two-dimensional ducts with rotational flow.

The transformed governing Eqs. (25–29) form a set of nonlinear equations on the (ξ, η) plane. Their numerical integration is carried out according to the following iterative scheme:

1) The velocity equation is linearized by assuming that the $\bar{\rho}$ and β distributions are known from the previous iteration level. Discretizing partial derivatives, employing central second-order accurate differencing (in subsonic flows), a system of algebraic equations with 9-diagonal banded nonsymmetric characteristic matrix is obtained. This is solved using the modified strongly implicit procedure.[21]

2) Once the meridional velocity field is determined, the transport equation for the drift function is integrated along streamlines (η = const lines) using a second-order accurate Runge-Kutta scheme. The newly calculated α distribution provides a better estimate for β, via Eq. (24). A better estimate for ρ is calculated from Eq. (6).

3) The geometry calculation is then performed by integrating Eqs. (27–29). Computational experience showed that inaccuracies associated with the error accumulation of the geometry calculation are minimized, if one determines the central streamline of the channel, η = const line first, and then starting from it, determines the inner and outer walls by integrating along ξ = const lines.

Iterations continue until velocity convergence is achieved. Convergence is established within 10^{-7} tolerance for the rms value of the velocity equation residual. Computational experiments showed that underrelaxing the velocity solution with a relaxation factor of the order of 0.4–0.5 and the geometry (r coordinate) with a relaxation factor of the order of 0.1 was necessary to both achieve and accelerate convergence.

Results and Discussion

The inverse design method proposed in this work has been validated for irrotational and rotational flows in two "reproduction" calculations. The term reproduction is used in the sense that, for a given geometry, a direct (analysis) code provides the boundary meridional velocity distributions that are then used by the inverse method to reproduce the original shape. The direct code employed for these computations is a reduced duct-flow version of a (ψ, ω) meridional code.[22]

Computational results for two "real-life" geometries, corresponding to the (nonbladed) annular duct of a two-stage axial compressor[23] and the duct of a radial compressor[24] are presented here. In both cases duct-flow computations were performed for subsonic irrotational and rotational flow conditions. The rotationality of the flow, when present, is due to a linear inlet meridional velocity profile, which in conjunction with the assumed uniform temperature and pressure profiles produces a compatible nonuniform total (stagnation) enthalpy

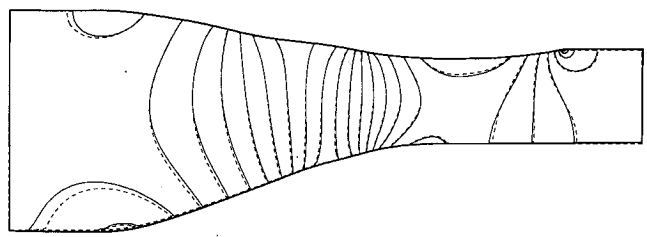

Fig. 1 Mach contours of inverse (——) and direct (---) method of axial compressor duct with irrotational flow (M_{min} = 0.135, ΔM = 0.015).

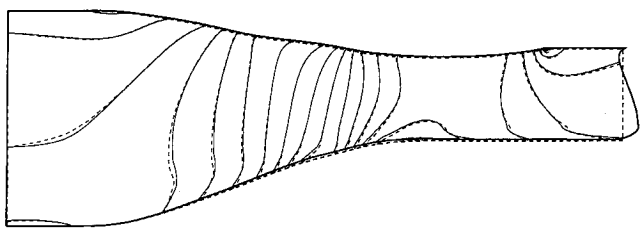

Fig. 2 Mach contours of inverse (——) and direct (---) method of axial compressor duct with rotational flow (M_{min} = 0.105, ΔM = 0.015).

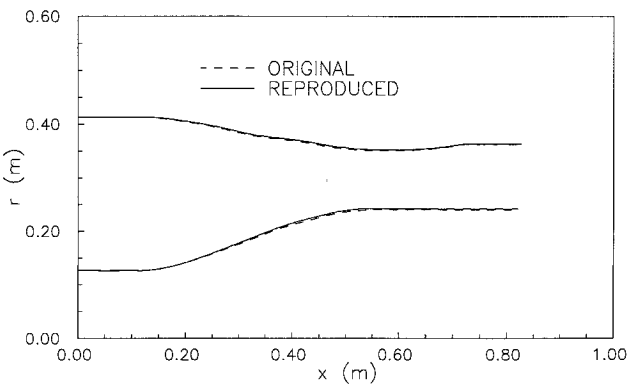

Fig. 3 Inner and outer wall geometries of axial compressor duct with rotational flow.

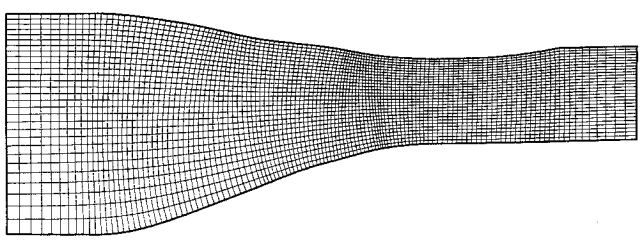

Fig. 4 Calculated grid of axial compressor duct with irrotational flow.

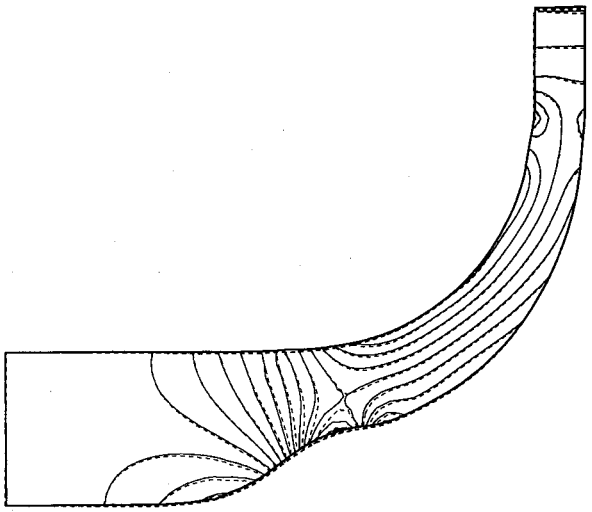

Fig. 5 Mach contours of inverse (——) and direct (---) method of radial compressor duct with irrotational flow (M_{min} = 0.15, ΔM = 0.015).

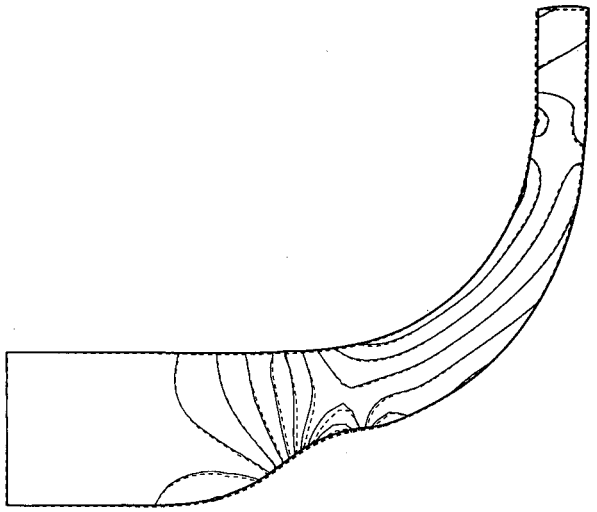

Fig. 6 Mach contours of inverse (——) and direct (---) method of axial compressor duct with rotational flow (M_{min} = 0.12, ΔM = 0.015).

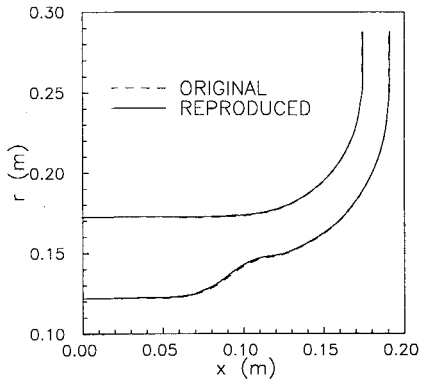

Fig. 7 Inner and outer wall geometries of radial compressor duct with rotational flow.

distribution. The inlet velocity variation was of the order of 30% and 10% for the axial and radial cases, respectively. For flow uniformity reasons, both geometries have been extended upstream and downstream. A 126 × 30 grid was used in both direct and inverse computations for the axial compressor duct, whereas a 70 × 20 grid was used for the radial compressor case. All inverse computations are initialized with a rectangular geometry, which is a severe test for the robustness of the numerical scheme, especially for the radial compressor case. Typically, 170 iterations are required for convergence using a 0.4 relaxation factor for the velocity field and a 0.1 factor for the radial coordinate field. The computational cost for the rotational case with the 126 × 30 grid is about 225 CPU seconds in one processor of an Alliant FX-80 machine.

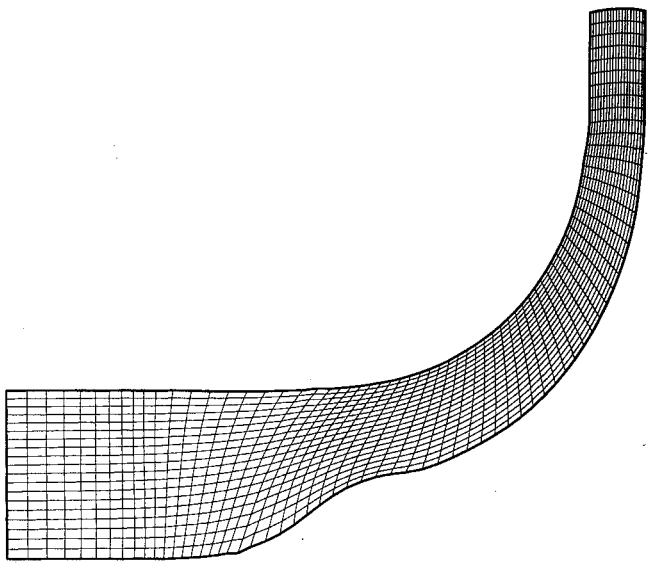

Fig. 8 Calculated grid of radial compressor duct with rotational flow.

Direct and inverse calculation results for the Mach number field along with the original (dashed lines) and reproduced (solid lines) geometries for the axial compressor duct with irrotational and rotational flow conditions are presented in Figs. 1 and 2, respectively. The agreement of the direct and inverse results is very good, although different grids and numerical schemes [(ψ, ω) formulation for the direct method and Clebsch formulation for the inverse one] have been employed.

In the rotational case, part of the incoming rotationality is introduced via a linear inlet swirl distribution (associated with a constant peripheral velocity distribution). The distorted outflow section observed in Fig. 2 is due to the irregular (ϕ, ψ) domain of integration. As it can be seen from Fig. 3, where the original and reproduced duct walls are compared in more detail, the outflow section distortion has almost no effect on the quality of the reproduction of the lateral solid boundaries. This is expected, since in the near-outflow region, streamwise gradients of all flow quantities are almost negligible.

The (ξ, η) grid produced by the inverse method for the irrotational axial compressor case is shown in Fig. 4. For irrotational flow conditions the (ξ, η) grid lines are potential and (meridional) streamlines, respectively. Note that in axisymmetric flows an equidistant grid in the ψ-wise sense, similar to the one employed in the present work, does not correspond to an equidistant grid with respect to the radial (Cartesian) coordinate. This is very clearly demonstrated in Fig. 4 where the calculated (ϕ, ψ) grid is coarser near the inner wall region.

Reproduction results for the radial compressor duct in terms of the Mach number field with irrotational and rotational flow conditions are presented in Figs. 5 and 6, respectively. The agreement between inverse (solid lines) and direct (dashed lines) method results is very good despite the facts that the mean curvature of the duct is quite high and that the grid employed is not fine enough (in the streamwise sense) to describe accurately the strong curvature changes observed along the inner wall.

A detailed comparison of the original and reproduced wall geometries for the radial compressor duct with rotational flow conditions is shown in Fig. 7. The corresponding (ξ, η) grid produced is included in Fig. 8. It is seen very clearly that in

the inner flow region grid lines, ξ = const and η = const lines are nonorthogonal. The inlet section, however, is indeed normal to the incoming flow that is implied by Eq. (32).

Conclusions

The development of an inverse method applicable to the design of axisymmetric channels with inviscid subsonic rotational flow has been described. Rotationality is due to incoming total enthalpy, entropy, and/or swirl nonuniformities that are transported downstream along meridional plane streamlines. The method is based on a potential/stream function formulation. The Clebsch transformation has been applied successfully, to decompose the meridional velocity vector into a potential and a rotational part using a drift function governed by a transport equation. An elliptic-type equation for the meridional velocity magnitude has been derived by treating the inverse problem as a geometric one on the (ϕ, ψ) plane. This equation and the drift transport equation that are coupled to the design geometry via the radial coordinate, are solved simultaneously using a simple iterative scheme. Calculated results for two real-life geometries concerning the nonbladed ducts of a two-stage axial compressor and that of a radial one are very satisfactory and indicate the reliability of the proposed design method.

References

[1]Lighthill, M. J., "A New Method of Two-Dimensional Aerodynamic Design," British Aeronautical Research Council R&M 2112, England, UK, 1945.

[2]Stanitz, J. D., "Design of Two-Dimensional Channels with Prescribed Velocity Distributions Along the Channel Walls," NACA Rept. 1115, 1953.

[3]Nelson, C. D., and Yang, T., "Design of Branched and Unbranched Axially Symmetrical Duct with Specified Pressure Distribution," *AIAA Journal*, Vol. 15, No. 9, 1977, pp. 1272–1277.

[4]Schmidt, E., "Computation of Supercritical Compressor and Turbine Cascades with a Design Method for Transonic Flows," *Journal of Engineering for Gas Turbines and Power*, Vol. 102, No. 1, 1980, pp. 68–74.

[5]Hawthorne, W. R., Wang, C., Tan, C. S., and McCune, J. E., "Theory of Blade Design for Large Deflections: Part I. Two-Dimensional Cascade," *Journal of Engineering for Gas Turbines and Power*, Vol. 106, No. 2, 1984, pp. 346–353.

[6]Bonataki, E., Chaviaropoulos, P., and Papailiou, K. D., "An Inverse Inviscid Method for the Design of Quasi-Three Dimensional Rotating Turbomachinery Cascades," *Proceedings of the 3rd International Conference on Inverse Design Concepts and Optimization in Engineering Sciences, ICIDES-III* (University Park, PA), edited by G. S. Dulikravich, 1991, pp. 189–200.

[7]Chaviaropoulos, P., Dedoussis, V., and Papailiou, K. D., "Compressible Flow Airfoil Design Using Natural Coordinates," *Computer Methods in Applied Mechanics and Engineering*, Vol. 110, 1993, pp. 131–142.

[8]Labrujere, T. E., "Review of Aerodynamic Design in the Netherlands," *Proceedings of the 3rd International Conference on Inverse Design Concepts and Optimization in Engineering Sciences, ICIDES-III* (University Park, PA), edited by G. S. Dulikravich, 1991, pp. 1–30.

[9]Joh, C.-Y., Grossman, B., and Haftka, R. T., "Design Optimization of Transonic Airfoils," *Proceedings of the 3rd International Conference on Inverse Design Concepts and Optimization in Engineering Sciences, ICIDES-III* (University Park, PA), edited by G. S. Dulikravich, 1991, pp. 445–456.

[10]Malone, J. B., and Swanson, R. C., "Inverse Airfoil Design Procedure Using a Multigrid Navier-Stokes Method," *Proceedings of the 3rd International Conference on Inverse Design Concepts and Optimization in Engineering Sciences, ICIDES-III* (University Park, PA), edited by G. S. Dulikravich, 1991, pp. 55–66.

[11]Dedoussis, V., Chaviaropoulos, P., and Papailiou, K. D., "A 3-D Inverse Methodology Applied to the Design of Axisymmetric Ducts," American Society of Mechanical Engineers Paper 92-GT-290, June 1992.

[12]Chaviaropoulos, P., Dedoussis, V., and Papailiou, K. D., "On the 3-D Inverse Potential Target Pressure Problem: Part I. Theoretical Aspects and Method Formulation," *Journal of Fluid Mechanics* (to be published).

[13]Labrujere, T. E., and Slooff, J. W., "Computational Methods for the Aerodynamic Design of Aircraft Components," *Annual Review of Fluid Mechanics*, Vol. 25, 1993, pp. 183–214.

[14]Dulikravich, G. S., "Aerodynamic Shape Design," Special Course on Inverse Methods for Airfoil Design for Aeronautical and Turbomachinery Applications, AGARD Rept. 780, May 1990.

[15]Lamb, H., *Hydrodynamics*, 6th ed., Dover, New York, 1945, p. 248.

[16]Dedoussis, V., Chaviaropoulos, P., and Papailiou, K. D., "Rotational Compressible Inverse Design Method for Two-Dimensional, Internal Flow Configurations," *AIAA Journal*, Vol. 31, No. 3, 1993, pp. 551–558.

[17]Stanitz, J. D., "A Review of Certain Inverse Methods for the Design of Ducts with 2- or 3-Dimensional Flow," *Applied Mechanics Review*, Vol. 41, No. 6, 1988, pp. 217–238.

[18]Dedoussis, V., Chaviaropoulos, P., and Papailiou, K. D., "On the 3-D Inverse Potential Target Pressure Problem: Part II. Numerical Aspects and Application to Duct Design," *Journal of Fluid Mechanics* (to be published).

[19]Aris, R., *Vectors, Tensors, and the Basic Equations of Fluid Mechanics*, Prentice-Hall, Englewood Cliffs, NJ, 1962, Chap. 7.

[20]Thompson, J. F., "Numerical Solution of Flow Problems Using Body-Fitted Coordinate Systems," *Computational Fluid Dynamics*, edited by W. Kollmann, Hemisphere, Washington, DC, 1980, pp. 1–98.

[21]Zedan, M., and Schneider, G. E., "A Three-Dimensional Modified Strongly Implicit Procedure for Heat Conduction," *AIAA Journal*, Vol. 21, No. 2, 1983, pp. 295–303.

[22]Kiousis, P., Chaviaropoulos, P., and Papailiou, K. D., "Meridional Flow Calculation Using Advanced CFD Techniques," American Society of Mechanical Engineers Paper 92-GT-325, June 1992.

[23]Rugger, R. S., and Benser, W. A., "Performance of a Highly Loaded Two-Stage Axial-Flow Fan," NASA TMX 3076, Aug. 1974.

[24]Bois, G., and Vouillarmet, A., "Analyse de l'Ecoulement Delivre par le Router d'un Compresseur Centrifuge," AIAAF, 21eme Colloque d'Aerodynamique Applique, Ecully, France, 1984.